A Method of Applying Linear Seakeeping Panel Pressure to Full Ship Structural Models

Ming Ma, DRS Defense Solutions, Stevensville/USA, mma@drs-ds.com
Chengbi Zhao, South China Univ. of Technology, Guangzhou/China, tccbzhao@scut.edu.cn
Nick Danese, Design Systems & Technologies, Antibes/France, ndar@ndar.com

Abstract

Panel based hydrodynamic analysis is well suited for transferring seakeeping loads to 3D FEM structural models. Because panel based hydrodynamic analysis is computationally expensive, and also not very sensitive to the mesh density, it is common to first calculate seakeeping loads from a coarser hydrodynamic mesh, and then to map the panel pressure and inertia loads to the corresponding finer structural model. Various interpolation methods have been proposed to map the loads from one mesh to another. While the pressure integration results in a perfect equilibrium in the hydrodynamic model, it is difficult to get a balanced structural model through any pressure interpolation methods. To re-balance the structural model, artificial accelerations and/or point loads have to be added. Malenica et al. (2008) proposed a method which maps the panel source strength instead of the panel pressure from a hydrodynamic mesh to the structural mesh, and then formulated the equations of motion in the structural mesh. The equations of motion also included a gravity term to account for the change in the coordinate system. The method results in a balanced structural model. In this paper, the cause of the unrealistic sway and surge force due to hydrostatic restoring pressure integration is explained. A method of applying linear seakeeping pressure loads is presented. The method differs from Bureau Veritas's approach in the following areas: 1. The corrective hydrostatic restoring force due to pressure integration is distributed to element nodes using quadratic programming; 2. There is no need to create and maintain two different models because the method only uses the structural mesh. A coarser hydrodynamic mesh is automatically generated from the structural mesh when the hydrodynamic analysis is performed; 3. The method is fully integrated within one FEA system, comprising modeling, loading, analysis, and evaluation.

1. Introduction

With the advent of new ship types, designs of increasingly larger scale, combined with their respective commercial service and/or military mission requirements, interest in using seakeeping loads for ship structural design has increased in recent years. Tools ranging from simple 2D strip theories to complex 3D CFD numerical simulation methods have been used for practical designs. Most seakeeping tools give hull girder loads (bending moments and shear forces). For tools with only sectional forces and moments available, we have recently proposed a method to transfer the sectional loads to 3D finite element models, *Ma et al. (2012)*. For tools with panel pressure available as an output, such as VERES (strip theory), WAMIT, HydroStar and PRECAL, it is desired to map panel pressure loads from a hydrodynamic model to the corresponding 3D finite element model, and to get a more realistic structural response. The hydrodynamic model is always balanced because the loads derived from a hydrodynamic analysis follow Newton's second law. When transferring hydrodynamic loads to a structural model, it is essential to maintain equilibrium in the structural model to ensure the loads are transferred correctly. However, because meshes for hydrodynamic analyses are often much coarser than the corresponding finite element model meshes, the structural model often becomes imbalanced after the panel pressure is mapped from the hydrodynamic mesh to the structural mesh. Until recently, most researchers have been focused on developing interpolation methods to directly map panel pressure from one mesh to another. Although various interpolation methods have been proposed and successfully used in design practice, accurately transferring seakeeping panel pressure loads to a finite element model still remains challenging. Often, the "inertia relief" method, *ABS (2010),* has to be used for the final adjustment to balance the structural model. The "inertia relief" technique is very powerful and can correct any imbalanced model. However, there are two shortcomings to this approach: (1) The additional inertial forces cause a change in the hull girder response (such as bending moment); (2) the change of the accelerations has to be relatively small to ensure the fictitious inertial forces do not significantly distort the original structural response. This often requires a visual inspection and engineering judgments. For the extreme load analysis (ELA), where the number of load cases is limited, visually inspecting each load case is possible. But for the spectral fatigue analysis (SFA), where there are thousands of load cases, it is not practical. *Malenica et al. (2008)* proposed a method which mapped the panel source strength instead of the panel pressure from a hydrodynamic mesh to the structural mesh, and then formulated the equations of motion in the structural mesh. A gravity force on the left side of the equations of motion accounts for the change in the coordinate system. This approach results in a perfectly balanced structural model without using “inertia relief.” In this paper, the additional gravity terms are derived from the integration of the hydrostatic restoring pressure. The cause of the unrealistic sway and surge force due to pressure integration is further explained and discussed. The corrective nodal forces are computed using quadratic programming, and applied to the wetted surface elements. Numerical examples are given for the validation.

2. General description of the potential problem

Consider a three-dimensional body of arbitrary shape in water of uniform depth. The amplitude of motions as well as of the incident waves are supposed to be small, while the fluid is assumed to be irrational, incompressible, and inviscid. As such, the ship motion problem may be formulated in terms of potential flow theory. Thus the fluid velocity vector may be represented by the gradient of a total velocity potential ψ, which is separated into two parts assuming a slender hull at slow forward speed:

$$\psi(x,y,z,t) = \Phi_s(x,y,z) + \phi_u(x,y,z)e^{i\omega t} \qquad (1)$$

Φ_s is a steady contribution due to forward speed U of the ship. ϕ_u is an unsteady part associated with the incident wave system and the unsteady body motion. $\omega = \omega_0 - Uk\cdot\cos\beta$ is the encounter frequency, which is related by the ship’s speed U, the incident wave frequency ω_0, the wave number $k = \omega_0^2/g$, and relative heading to the incident wave direction β. With the assumption of small oscillations, the total unsteady velocity field (ϕ_u, which varies during one oscillation) around the ship can be divided into a series of independent velocity potentials: incident wave $\phi_0(x,y,z,t)$ component, diffracted wave $\phi_7(x,y,z,t)$ component and six radiation wave $\phi_j(x,y,z,t)$ components for the six degrees of ship motions.

$$\phi_u e^{i\omega t} = \left[\phi_0 + \phi_7 + \sum_{j=1}^{6}\phi_j\right]e^{i\omega t} = A\left[\varphi_0 + \varphi_7 + \sum_{j=1}^{6}\xi_j\varphi_j\right]e^{i\omega t} \qquad (2)$$

In the case of long crested, harmonic progressive waves the incident potential for infinite deep water is defined as, $\varphi_0 = (ig/\omega_0)e^{k(z - ix\cos\beta - iy\sin\beta)}$. The steady velocity can be separated into different terms as well. It is common practice to assume that there is a base flow, either the double-body flow or the uniform flow, and a small steady disturbance potential which is linear in forward speed.

$$\Phi_s(x,y,z) = -Ux + \varphi(x,y,z) \qquad (3)$$

The individual potentials must satisfy the following conditions:

Table 1: Boundary value problems (BVP) of the potential flows

	Steady	Radiation	Diffraction
In the fluid	$\nabla^2\Phi_s = 0$	$\nabla^2\varphi_j = 0$	$\nabla^2\varphi_7 = 0$
Free surface	$\frac{\partial\Phi_s}{\partial z} = 0$	$\frac{\partial\varphi_j}{\partial z} - k\varphi_j = 0$	$\frac{\partial\varphi_7}{\partial z} - k\varphi_7 = 0$
Body	$\frac{\partial\Phi_s}{\partial n} = 0$	$\frac{\partial\varphi_j}{\partial n} = i\omega n_j + m_j$	$\frac{\partial(\varphi_0 + \varphi_7)}{\partial n} = 0$
Bottom	$\frac{\partial\Phi_s}{\partial n} = 0$	$\frac{\partial\varphi_j}{\partial n} = 0$	$\frac{\partial\varphi_7}{\partial n} = 0$

where
$\vec{r} = (x, y, z)^T$
$\vec{n} = (n_1, n_2, n_3)^T$
$(n_4, n_5, n_6)^T = \vec{r} \times \vec{n}$
$(m_1, m_2, m_3)^T = -(\vec{n} \cdot \nabla)\nabla\Phi_S$
$(m_4, m_5, m_6)^T = -(\vec{n} \cdot \nabla)[\vec{r} \times \nabla\Phi_S] = \vec{r} \times (m_1, m_2, m_3)^T - \vec{n} \times \nabla\Phi_S$

These BVP-s are all solved using the Boundary Integral Equation (BIE) technique based on the Kelvin type of Green function. The source formulation is used, so that the velocity potentials are represented by the source distribution over the wet part of the body. The double body potential is:

$$\varphi(p) = \oiint_B G_0(p, q)\, \sigma(q)\, ds \tag{4}$$

and the radiation and diffraction potential is :

$$\varphi_j(p) = \oiint_B G(p, q)\, \sigma_j(q)\, ds + \frac{U^2}{g} \oint_{WL} G(p, q)\, \sigma_j(q) n_1\, dl \qquad j = 1, \dots, 7 \tag{5}$$

S represents the outer wet part of the ship, σ is the panel source strength, G_0 is the simple Green function, and G is the Kelvin type of Green function. The source strength σ of each potential can be determined by the following boundary integral equation:

Double body potential:

$$2\pi\sigma(p) + \oiint_B \frac{\partial G_0(p, q)}{\partial n} \sigma(q)\, ds = n_1 U \tag{6}$$

Radiation potential:

$$2\pi\sigma_j(p) + \oiint_B \frac{\partial G(p, q)}{\partial n} \sigma_j(q)\, ds + \frac{U^2}{g} \oint_{WL} G(p, q)\, \sigma_j(q) n_1 dl = i\omega n_j + m_j \qquad j = 1, \dots, 6 \tag{7}$$

Diffraction potential:

$$2\pi\sigma_7(p) + \oiint_B \frac{\partial G(p, q)}{\partial n} \sigma_7(q) ds + \frac{U^2}{g} \oint_{WL} G(p, q)\, \sigma_7(q) n_1 dl = -\frac{\partial \varphi_0}{\partial n} \tag{8}$$

Eqs. (6) to (8) are solved by usual numerical routines after discretizing the body surface in a finite number of flat panels. Once the potentials are obtained, the pressure of the wetted body surface can be calculated by Bernoulli's equation:

$$p = -\rho\left(\frac{\partial \psi}{\partial t} + \frac{1}{2}\nabla\psi \cdot \nabla\psi - \frac{1}{2}U^2 + gz\right) \tag{9}$$

Ignoring higher order terms, the pressure at a position of the body can be expanded into a Taylor series around the mean position, H_0: $p_H = p_{H_0} + \vec{a}\nabla p_{H_0} = p_S + p_u$, in which

$$p_S = -\rho\left(\frac{1}{2}\nabla\Phi_S \cdot \nabla\Phi_S - \frac{1}{2}U^2 + gz\right) \tag{10}$$

$$p_u = -\rho\left(\frac{\partial \phi_u}{\partial t} + \nabla\Phi_S \cdot \nabla\phi_u\right) - \rho(\vec{a} \cdot \nabla)\left(\frac{\nabla\Phi_S \cdot \nabla\Phi_S}{2} + gz\right) \tag{11}$$

$\vec{a} = \vec{\xi} + \vec{\Omega} \times \vec{r}$. The unsteady force and moment due to the oscillatory motion are obtained by integrating the unsteady component of the pressure p_u over the wetted surface:

$$H_j(t) = \iint_B p_u n_j\, ds = e^{i\omega t}\left[X_j + \sum_{k=1}^{6} \xi_k \left(\omega^2 a_{jk} - i\omega b_{jk} - c_{jk}\right)\right] \qquad j = 1, \dots, 6 \tag{12}$$

Here the integration is over the mean position of the hull surface. The equations of motion that govern the steady-state time-harmonic response of the body follow from Newton's second law:

$$H_j(t) = -\omega^2 e^{i\omega t} \sum_{k=1}^{6} M_{jk}\, \xi_k \qquad j = 1, \dots, 6 \tag{13}$$

$\xi_j = \xi_R + i \cdot \xi_I$ is the motion RAO. M_{kj} is the body mass matrix. Combining equation (12) and (13), the response amplitude operator RAO can be determined by the linear equation system,

$$\sum_{k=1}^{6} \left[-\omega^2 \left(M_{jk} + a_{jk}\right) + i\omega b_{jk} + c_{jk}\right]\xi_k = X_j \qquad j = 1, \dots, 6 \tag{14}$$

a_{kj} and b_{kj} are the added mass and damping coefficient which originate from the radiation potential. X_j is the exciting force due to the incident and diffracted wave potential. a_{kj}, b_{kj} and X_j are derived from the first term of (11) and depend on both the forward speed and the frequency of oscillation.

$$a_{kj} = -\frac{\rho}{\omega^2}\mathrm{Re}\left[\iint_B \left(i\omega\varphi_j + \nabla\Phi_s \cdot \nabla\varphi_j\right) n_k \, ds\right] \qquad k,j = 1, \dots, 6 \tag{15}$$

$$b_{kj} = \frac{\rho}{\omega}\mathrm{Im}\left[\iint_B \left(i\omega\varphi_j + \nabla\Phi_s \cdot \nabla\varphi_j\right) n_k \, ds\right] \qquad k,j = 1, \dots, 6 \tag{16}$$

$$X_j = -\rho \iint_B \left[i\omega(\varphi_0 + \varphi_7) + \nabla\Phi_s \nabla(\varphi_0 + \varphi_7)\right] n_j ds \qquad j = 1, \dots, 6 \tag{17}$$

The restoring coefficient c_{kj} is derived from the second term of (11). It is a function of the forward speed, the gradient of the hydrostatic pressure, and the steady dynamic pressure field. The restoring coefficient is given as:

$$c_{kj} = -\rho \iint_B \left[(\vec{\alpha} \cdot \nabla)\left(\frac{1}{2}\nabla\Phi_s \cdot \nabla\Phi_s + gz\right)\right] n_k \, ds \qquad k,j = 1, \dots, 6 \tag{18}$$

The ship hull girder cross section shear forces and bending moments, including wave induced pressure loads and inertial loads, are:

$$F_j = \iint_B p_u n_j ds - \omega^2 \sum_{k=1}^{6} M_{jk} \xi_k \qquad j = 1, \dots, 6 \tag{19}$$

F_1, F_2 and F_3 are the force components in the x, y and z directions. F_4, F_5 and F_6 are the moments about the x, y and z axes, Fig.1.

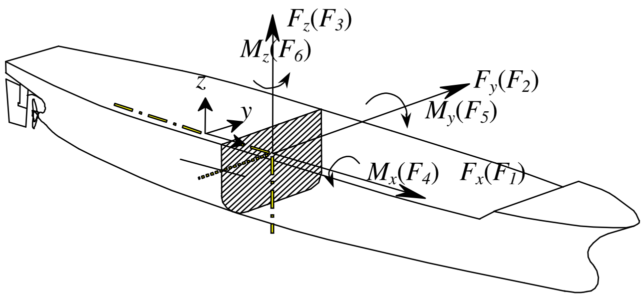

Fig. 1: Convention for wave loads caused by oscillatory motions

3. Applying pressure loads to a finite element model

For a floating structure, it is important to obtain equilibrium before performing a finite element analysis. An imbalanced model causes an unrealistic result. Panel based hydrodynamic analysis is well suited for transferring hydrodynamic panel pressure to 3D finite element structural models. However, because meshes for hydrodynamic analyses are often much coarser than the corresponding finite element model meshes, it is necessary to map panel pressure from one mesh to another. While a hydrodynamic model is always in equilibrium, the corresponding structural model with a direct load mapping is usually not balanced. To transfer linear seakeeping pressure to a 3D finite element model while maintaining the model's equilibrium, the following procedure can be used.

1. Construct discretized boundary integral equations (6), (7) and (8) based on the hydrodynamic model mesh, and obtain the panel source strength of each potential.
2. Map the panel source strength from the hydrodynamic mesh to the corresponding structural mesh.

3. Compute hydrodynamic added mass, damping, and restoring coefficients by integrating the finite element wetted surface panels.
4. Construct the equations of motion based on the wetted surface mesh of the finite element model, and obtain the motion RAOs.
5. Compute the finite element panel pressure and the corrective hydrodynamic restoring nodal forces.
6. Apply the panel pressure and the corrective hydrodynamic restoring nodal forces to the finite element model. The finite element model is now in perfect equilibrium.

3.1 Hydrostatic restoring loads

When the vessel oscillates, hydrostatic restoring forces, caused by heave, roll and pitch motion, will be present. We have to calculate these pressure contributions on the instantaneous hull wetted surface. This means on an oscillating surface *H*, as shown in Fig.2(a). To circumvent the non-linearity of the pressure integration, the pressures are evaluated on the known mean wetted surface of the vessel H_0, as shown in Fig.2(b)

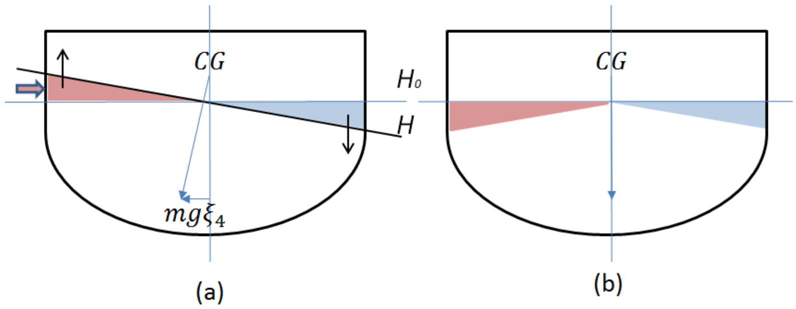

Fig. 2 Hydrostatic restoring force

The hydrostatic restoring force matrix, also called the hydrostatic "stiffness" matrix, is commonly expressed in basic hydrostatic properties, such as waterplane area, displacement, transverse metacenter, etc. For example, for a symmetric model, the matrix is given as the following:

$$[C] = \rho g \begin{bmatrix} 0 & 0 & 0 & 0 & 0 & 0 \\ 0 & 0 & 0 & m/\rho & 0 & 0 \\ 0 & 0 & A_w & 0 & -M_w & 0 \\ 0 & 0 & 0 & \Delta GM_T & 0 & 0 \\ 0 & 0 & -M_w & 0 & I_w & 0 \\ 0 & 0 & 0 & 0 & 0 & 0 \end{bmatrix} \tag{20}$$

A_w, M_w, *and* I_w are the area, moment, and moment of inertia of the water plane about the Y-axis, Δ is the displacement of ship, GM_T is the transverse metacentric height. Note that the small lateral forces, c_{24} and c_{15} of matrix (18), caused by roll and pitch motion respectively, are balanced by the gravity component, as illustrated by Fig.2(a). Hydrostatic restoring matrix (20) has been successfully and widely used in many seakeeping numerical tools. The elemental restoring force can be obtained by

$$R_j = \sum_{k=1}^{6} c_{jk}\xi_k \qquad j = 1, \dots, 6 \tag{21}$$

Eq.(21) can be used to compute hull girder sectional loads and the element nodal forces of a finite element model. The coefficient of matrix (20) can also be obtained by integrating the restoring pressure over the wetted body surface. The hydrostatic restoring pressure is given in the second term of Eq.(11) as,

$$p_r = -\rho(\vec{a}\cdot\nabla)\left(\frac{\nabla\Phi_s\cdot\nabla\Phi_s}{2} + gz\right)$$

Ignoring second order terms,

$$p_r = -\rho(\vec{a}\cdot\nabla)(gz) = -\rho g a_3 = -\rho g(\xi_3 + \xi_4 y - \xi_5 x) \tag{22}$$

The restoring forces due to the vessel oscillations are:

$$C_j = \iint_B p_r n_j ds = \rho g \iint_B (\xi_3 + \xi_4 y - \xi_5 x) n_j ds \qquad j = 1,\dots,6 \tag{23}$$

Expanding (23), we have

$$c_{11} = c_{22} = 0$$
$$c_{33} = \rho g \iint_B (\xi_3) n_3 ds = \rho g \xi_3 \iint_B n_3 ds = \rho g \xi_3 A_w$$
$$\dots$$
$$c_{24} = \rho g \iint_B (\xi_4 y) n_2 ds = \rho g \xi_4 V_y = \Delta\xi_4 = mg\xi_4$$
$$c_{15} = \rho g \iint_B (-\xi_5 x) n_1 ds = -\rho g \xi_5 V_x = -\Delta\xi_5 = -mg\xi_5$$

The hydrostatic restoring force matrix, derived from pressure integration, is:

$$[\overline{C}] = \rho g \begin{bmatrix} 0 & 0 & 0 & 0 & -m/\rho & 0 \\ 0 & 0 & 0 & m/\rho & 0 & 0 \\ 0 & 0 & A_w & 0 & -M_w & 0 \\ 0 & m/\rho & 0 & \Delta GM_T & 0 & 0 \\ -m/\rho & 0 & -M_w & 0 & I_w & 0 \\ 0 & 0 & 0 & 0 & 0 & 0 \end{bmatrix} \tag{24}$$

The coefficient c_{24} and c_{15} of $[\overline{C}]$ are no longer zero when the hydrostatic restoring pressure is evaluated on the known mean wetted surface H_0. This implies that the pressure integration over the wetted body surface would result in additional sway and surge forces, and these additional sway and surge forces will cause imbalanced force and moment for the finite element model. To offset the unrealistic sway and surge forces caused by linear theory assumption, *Malenica et al. (2008)* proposed a method to add gravity terms to the left side of the equation of the motions (14). The additional gravity terms are equivalent to setting c_{24} and c_{15} to be 0. With the correction of the gravity force, the hydrodynamic restoring coefficient matrix (24), obtained from the pressure integration, becomes the matrix (20), which is derived from the traditional hydrostatic method. The gravity force was then distributed to the whole finite element model to balance the sway and surge forces due to pressure integration. Because the additional hydrostatic restoring force due to pressure integration is acting on the wetted surface, it may be more logical to make the nodal force adjustment on the wetted surface element rather than the whole ship. In the following section, a method of using quadratic programming to find the corrective nodal forces is presented.

3.2 Adjusting imbalanced forces using quadratic programming

To apply the hydrostatic restoring pressure to a finite element panel, a set of fictitious nodal forces have to be added to the element to counteract the unrealistic sway and surge force due to pressure integration.

$$R_j - C_j = 0 \qquad j = 1,\dots,6 \tag{25}$$

There are a number of ways to assign elemental nodal forces to get desired resulting forces and moments. One of the approaches is to use the quadratic programming method, *Fletcher (1987)*. The objective function is to minimize the magnitude of the nodal forces, which is given by,

$$\textbf{minimize}: q = \sum_{k=1}^{m} \left(f_{x_k}^2 + f_{y_k}^2 + f_{z_k}^2 \right) \tag{26}$$

k is the node index of the panel, and m is the number of nodes of a panel. f_{x_k} , f_{y_k} , and f_{z_k} are the finite element nodal force. The constraints are the six restoring forces and moments, as defined in Eq.(27):

$$\begin{aligned}
&\sum_{k=1}^{m} f_{x_k} = R_1 - C_1 \\
&\sum_{k=1}^{m} f_{y_k} = R_2 - C_2 \\
&\sum_{k=1}^{m} f_{z_k} = R_3 - C_3 \\
&\sum_{k=1}^{m} \left(- f_{y_k}(z_k - z_c) + f_{z_k}(y_k - y_c)\right) = R_4 - C_4 \\
&\sum_{k=1}^{m} \left(- f_{z_k}(x_k - x_c) + f_{x_k}(z_k - z_c)\right) = R_5 - C_5 \\
&\sum_{k=1}^{m} \left(- f_{x_k}(y_k - y_c) + f_{y_k}(x_k - x_c)\right) = R_6 - C_6
\end{aligned} \tag{27}$$

x_c, y_c, and z_c describe the location of the center of gravity. x_k, y_k, and z_k are the finite element nodal location. R_j is the panel restoring force ($j=1,\ 2,$ and 3) and moment ($j=4,\ 5,$ and 6) obtained from Eq.(21). C_j is the panel restoring force and moment using pressure integration in Eq.(23). Eqs.(26) and (27) can be rewritten as

$$minimize:\ q(\boldsymbol{X}) = \frac{1}{2}\boldsymbol{X}^T G \boldsymbol{X} \tag{28}$$

$$subject\ to:\ A^T \boldsymbol{X} = b \tag{29}$$

$G=2I$, $\boldsymbol{X}$ is a vector of the corrective finite element model's nodal forces, $\boldsymbol{A}$ is the matrix of the linear equality constraint coefficient, and $\boldsymbol{b}$ is a vector of the difference between the elemental forces and moments obtained by the traditional method and by the pressure integration method. The quadratic programming problem can be solved by the method of Lagrangian multipliers. The Lagrangian function becomes:

$$L(\boldsymbol{X},\boldsymbol{\lambda}) = \frac{1}{2}\boldsymbol{X}^T \boldsymbol{G}\boldsymbol{X} - \boldsymbol{\lambda}^T(\boldsymbol{A}^T\boldsymbol{X} - \boldsymbol{b}) \tag{30}$$

and the stationary point condition yields the equations

$$\begin{bmatrix} G & -A \\ -A^T & 0 \end{bmatrix} \begin{Bmatrix} X \\ \lambda \end{Bmatrix} = -\begin{Bmatrix} 0 \\ b \end{Bmatrix} \tag{31}$$

For a quadrilateral (triangular) element, the number of variables in Eq.(31) is $4(3)\times 3+6$, so the solution is very fast.

4. Integration to the structural analysis

The linear seakeeping model based on presented theory is implemented as a plugin component, MAESTRO-Wave, for the software suite MAESTRO, www.maestromarine.com, Fig.3. MAESTRO is a structural design tool specifically tailored to suit naval architects and their finite element analysis and limit-state (failure mode) evaluation needs. Unlike many other seakeeping tools, where end users need to use multiple graphical user interfaces (GUIs) to perform seakeeping analysis and then transfer the seakeeping loads to a different tool for a structural analysis, MAESTRO-Wave is seamlessly integrated into MAESTRO through a single Windows-based GUI that completely encompasses the structural modeling (preprocessing), the ship-based loading (including seakeeping loads), the finite element analysis, the limit-state evaluation, and the post-processing. MAESTRO-Wave leverages the

MAESTRO model's wetted panel definition, evaluation patch definition, tank definition and weight distribution, and then generates a database of regular unit wave responses, which include ship motions, accelerations and dynamic pressure acting on the hull for each speed, heading and wave frequency. MAESTRO-Wave uses three different wetted panel discretization methods; the original finite element mesh, the evaluation patch mesh, and the section based re-panelization mesh, for the linear seakeeping analysis. The original finite element mesh is applicable when the number of wetted elements is less than 3000. In this approach, a source strength is computed for each finite element panel, and the seakeeping analysis mesh is the same as the finite element mesh. When the number of wetted elements is greater than 3000, super-element methods are recommended. A super-element consists of many actual finite elements. The elements in a super-element have the same source strength. However, the pressure of each finite element panel is different because the velocity potentials depend on not only the source strength, but also the element location. There are two super-element methods can be selected in MAESTRO-Wave; the evaluation patch method and the section based re-panelization method. The evaluation patch method leverages MAESTRO's existing structural failure mode evaluation framework, where each evaluation patch is automatically defined based on the boundary of bulkheads, stiffeners and frames, Fig.4. The second super-element method uses the section cuts of the wetted surface mesh to generate a new set of coarse panels. Once the unit wave hydrodynamic load database is available, either by using MAESTRO-Wave or third party tools such as PRECAL and VERES, the hull girder load response RAOs, such as vertical bending moment, shear force and torional moment, as well as the element stress RAOs, can be obtained. The short-term and long term design waves can be generated by the hull girder dominant load parameters, wave scatter diagrams, wave spectra and the return period. The structure spectral fatigue life can be determined by the element stress response RAO. Figs.5 and 6 illustrate the procedures of the extreme load analysis and the spectral fatigue analysis.

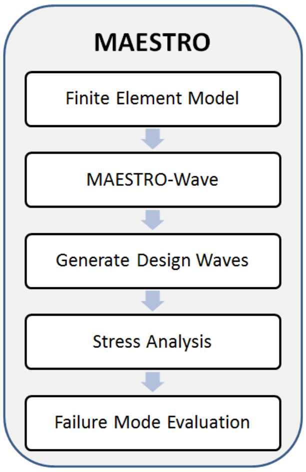

Fig.3: Process flow in MAESTRO

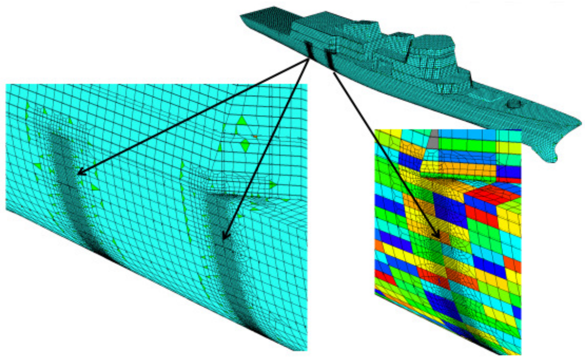
Fig.4: Evaluation patch

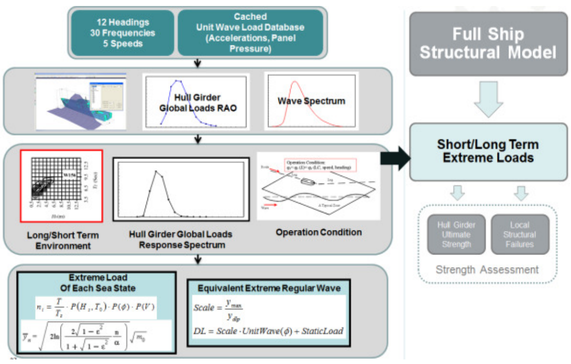

Fig. 5: Extreme load analysis

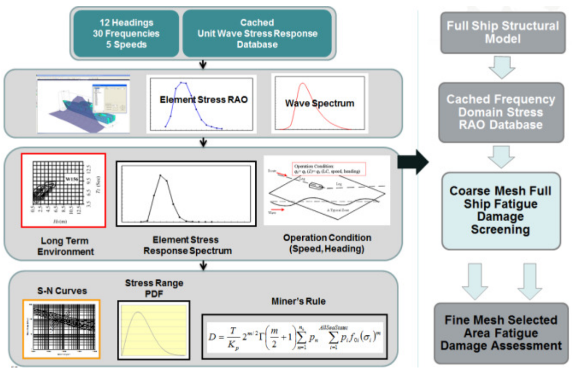

Fig. 6: Spectral fatigue analysis

5. Numerical Validation

The S-175 container ship is standard ITTC test case for wave-induced motions and structural loads, *ITTC (2010)*. The database that resulted from that study includes numerical results from many institutions, and also some experimental data. Table 2 lists the main particulars.

Table 2: Main particulars of the S175 container ship

Length between perpendiculars	175.00 m
Breadth	25.40 m
Depth	15.40 m
Draught	9.50 m
Displacement	24742 t
LCG aft of midship	2.50 m
Block coefficient	0.572
Midship section coefficient	0.98
XG(from AP)	84.97 m
YG(from centerline)	0.00 m
R_{xx}	9.652
R_{yy}	42.07
R_{zz}	43.17

Three hydrodynamic analyses are conducted for the comparison. For the first analysis, labeled "MAESTRO-Wave" in the following result figures, the hydrodynamic mesh is the same as the finite element mesh, Fig.7(a). For the second analysis, labeled "MAESTRO-Wave (Coarse Mesh)," the hydrodynamic mesh is coarser than the finite element mesh, Fig.7(b). The first two models were analyzed using MAESTRO-Wave. The third model was analyzed using PRECAL6.6 of MARIN.

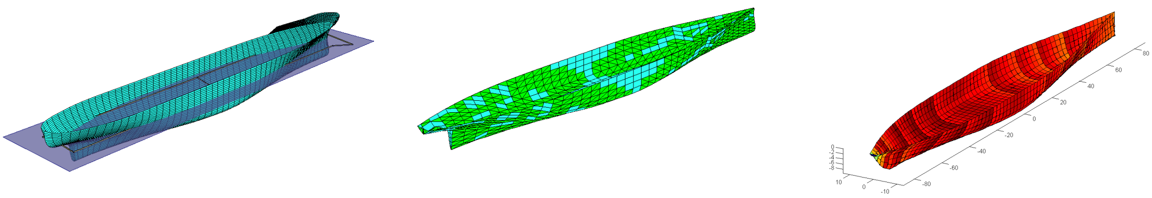

(a)MAESTRO-Wave (b)MAESTRO-Wave(Coarse Mesh) (c)PRECAL

Fig. 7: Seakeeping model mesh

The ship is advancing with constant speed v=22.145 knots with four different headings, β=0°, β=90°, β=120° and β=180°. All results are presented in a non-dimensional way using wave amplitude A, wave number k, encounter frequency ω, water density ρ, gravitational acceleration g, ship beam B and ship length between perpendiculars L_{pp} as given in Table 3.

Table 3: Non-dimensional parameter definition

Translational motions (heave, sway and surge)	$x' = x\frac{1}{A}$
Rotational motions (roll, pitch and yaw)	$\theta' = \theta\frac{1}{kA}$
Bending moments	$M' = M\frac{1}{\rho g B L_{pp}^2 A}$
Shear forces	$F' = F\frac{1}{\rho g B L_{pp} A}$

The motion and load RAO results, along with the available experiment data from ITTC, are shown in Figs. 8 to 12.

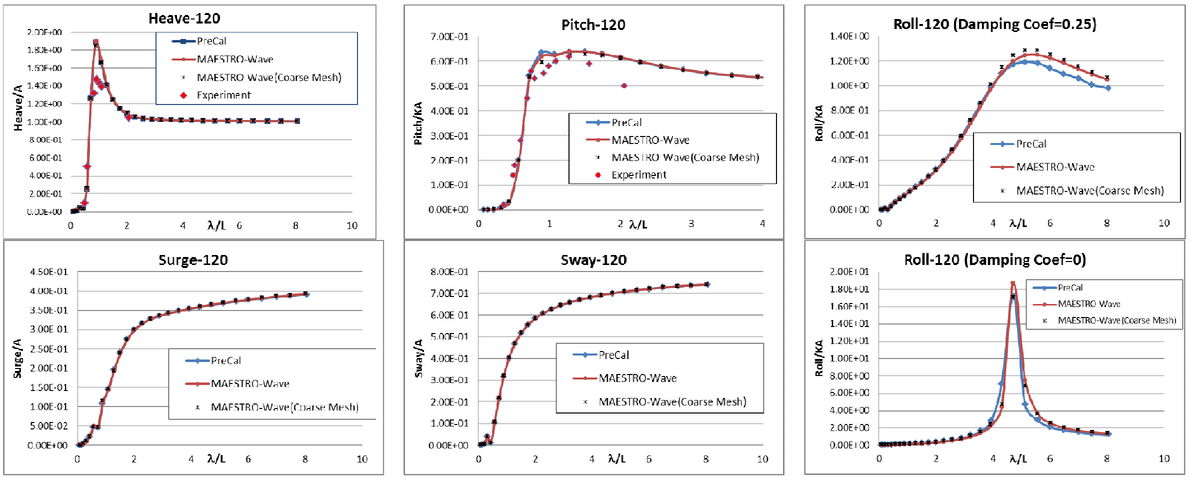

Fig. 8: Motion RAO (β=120°, F_r=0.275)

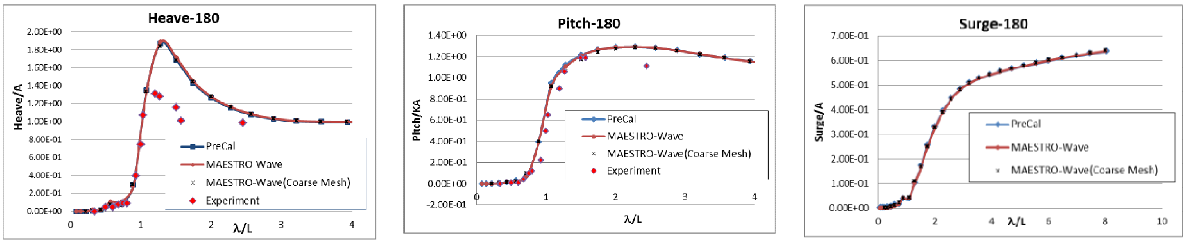

Fig. 9: Motion RAO (β=180°, F_r=0.275)

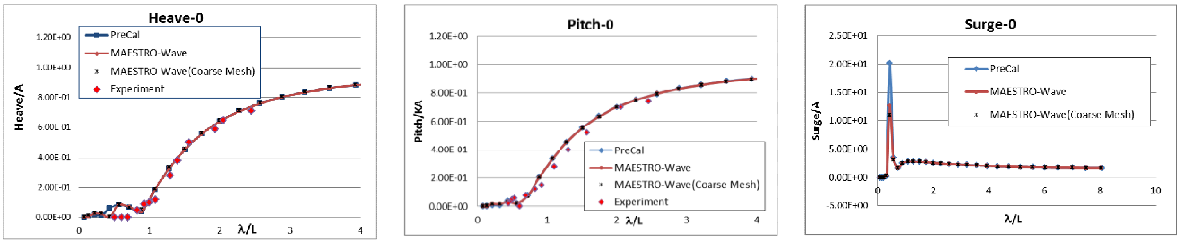

Fig. 10: Motion RAO (β=0°, F_r=0.275)

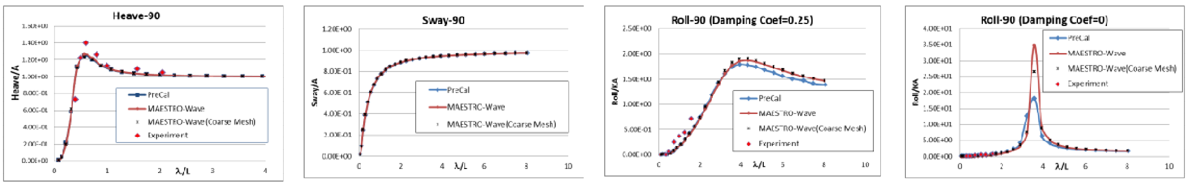

Fig. 11: Motion RAO (β=90°, F_r=0.275)

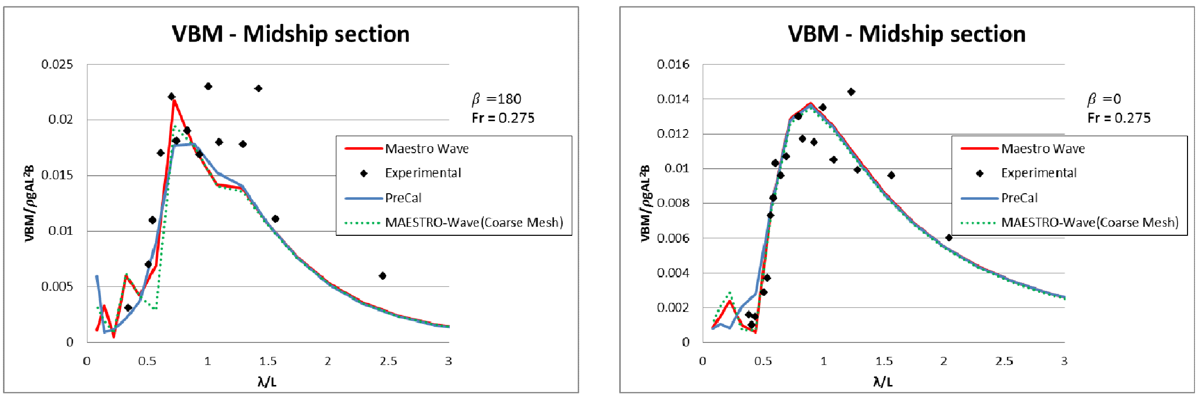

(a) β = 180° (b) β = 0°

Fig. 12: Vertical bending moment RAO (F_r=0.275)

6. Case study

To illustrate a complete procedure of using linear seakeeping pressure load for a structural analysis, including generating design waves, a full ship example is given in this section. A finite element model was provided by NAPA Ltd of a nominal frigate (L_{pp} = 150 m, Δ =4000 t). The model was created using NAPA-Steel as a molded form structural model, Fig.13(a). The NAPA-Steel/MAESTRO interface program can generate a full ship finite element mesh in MAESTRO format from a molded form structural model with one click of a button. The generated finite element model has over 61,000 nodes and 125,000 elements, Fig.13(b). This interface program also automatically translates the compartment and wetted surface definitions as MAESTRO groups, Fig.13(c) and (d). In addition, the weight distribution, tank loads and floating condition defined in the NAPA hydrostatic module are translated into MAESTRO. With a complete finite element mesh and load definition, the generated finite element model is ready for a linear static analysis without any additional manual editing.

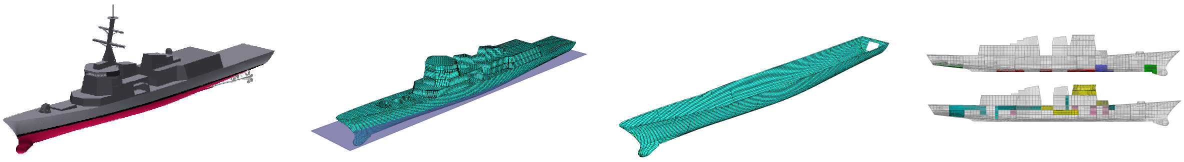

(a)Molded form model (b)Finite element model (c) Wetted surface elements (c)Tank definition

Fig. 13: NAPA-Steel generated finite element model

Once the finite element model and the weight distribution are imported (or constructed), MAESTRO will first perform a hydrostatic balance to obtain the mean draft plane and to identify the wetted surface elements. Next, a seakeeping analysis is performed by executing MAESTRO-Wave. It is assumed the ship has a forward speed of 20 knots, 7 different headings, and 30 frequencies. A unit wave response database is generated. The database includes wave-induced accelerations, panel pressures, nodal forces due to hydrostatic restoring correction, and the cross sectional hull girder loads. The unit wave pressure distribution, ship motion RAOs, and hull girder load RAOs can be displayed for sanity checks.

Table 4: Combined dynamic and static loads and the structural responses

	Hogging	Sagging
Static and dynamic pressure	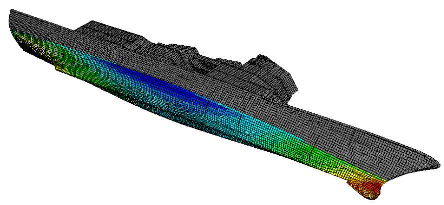	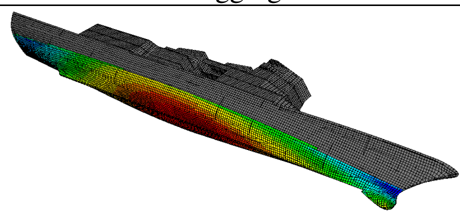
Vertical bending moment distribution	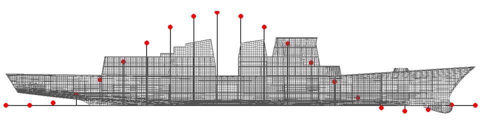	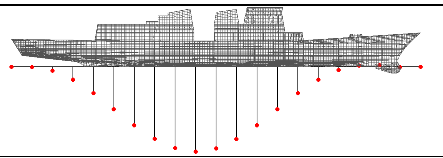
Vertical shear force distribution	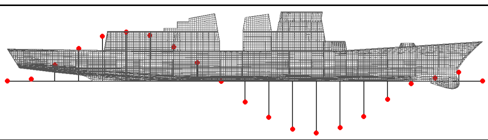	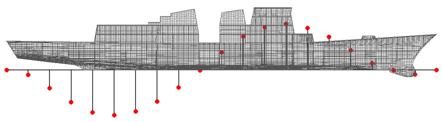
Longitudinal stress and deformation	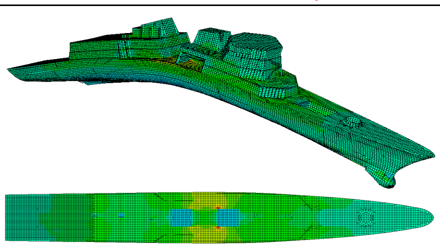	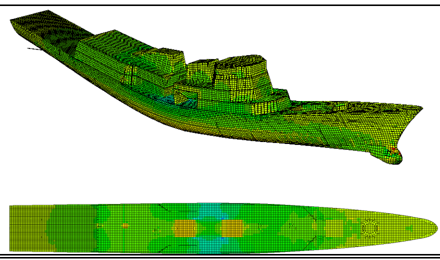

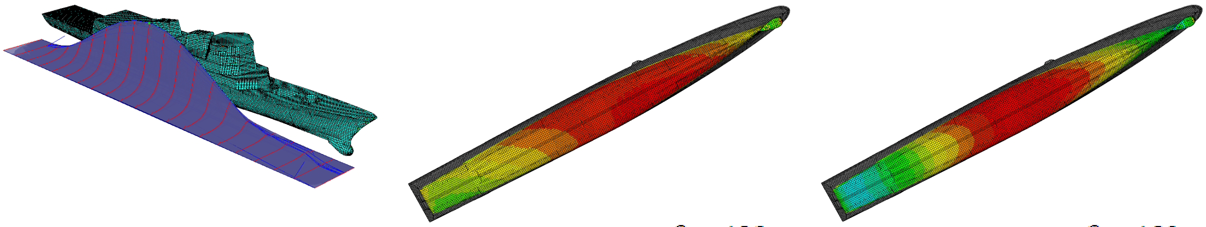

(a)VBM RAO of all stations (b)Pressure distribution $\beta = 120°$ (b)Pressure distribution $\beta = 180°$

Fig. 14: Vertical bending moment RAO and unit wave pressure distribution

Figure 14(a) shows the hull girder vertical bending moment RAO of all sections. The closure of the bending moment for all frequencies indicates the model is indeed in equilibrium. Note that the hull girder loads reported in MAESTRO, such as vertical bending moment, vertical shear force, horizontal bending moment, horizontal shear force and longitudinal torsional moment, are derived from the basic loads (such as panel pressure and inertia force), and they are computed solely for the purpose of verifying the integrity of individual load components. A design wave is generated based on a desired dominant load parameter (DLP), a sea state diagram and the return period. The dynamic design wave, which has a perfect equilibrium based on the presented method, combined with the static loads, becomes a regular static analysis load case. Table 4 shows the combined dynamic and static panel pressure, hull girder bending moment and shear force distribution, and the deformation responses of the model under sagging and hogging loads.

7. Concluding remarks

This paper discussed two key issues of applying linear seakeeping pressure loads to 3D finite element models. In order to get a perfect equilibrium of a finite element structural model, the source strength, but not the element pressure, should be mapped from the hydrodynamic mesh to the structural mesh. The equations of motions should be constructed in the structural mesh. Secondly, the unrealistic sway and surge forces due to hydrostatic restoring pressure integration should be corrected. The correction can be done either through distributing the gravity force to the whole model, or applying the corrective nodal forces to the wetted element using the proposed quadratic programming method. The proposed method is validated by comparing PRECAL of MARIN.

Acknowledgments

The authors thank Tomi Holmberg of NAPA Group for providing the finite element model presented in this paper.

References

ABS (2010), *Guide for 'Dynamic Loading Approach' for floating production, storage and offloading (FPSO) installations*, American Bureau of Shipping

FLETCHER, R. (1987), *Practical Methods of Optimization*, 2nd Ed., John Wiley & Sons

ITTC (2010), *Comparative study on linear and nonlinear ship motion and loads*, ITTC workshop on seakeeping, Seoul

MA, M.; HUGHES, O.; ZHAO, C.B. (2012), *Applying sectional seakeeping loads to full ship structural models using quadratic programming*, ICMT2012, Harbin

MALENICA, S.; STUMPF, E.; SIRETA, F.X.; CHEN, X.B. (2008), *Consistent hydro-structure interface for evaluation of global structural responses in linear seakeeping*, OMAE08, Estoril